Original Article

Analysis of the magnetic susceptibility of armchair nanoribbon in the presence of magnetic field

Sorgul Kashmiri[1*], Wahidullah Enayat[2]

[1] Assistant Profesor, Lecturer in Physics Department of Education Faculty, Balkh University, E-mail: sorgul.kashmiri@gmail.com

[2]Senior Teaching Assistant, Lecturer in Physics Department of Education Faculty, Samangan University, E-mail: wahidullahenayat@smgu.edu.af

***Correspondence:** Sorgul kashmiri

ABSTRACT

Objective: Nanotechnology has been a promising area of social, environmental, and financial benefits. The present study aims to investigate the temperature behavior of magnetic susceptibility of the grapheme armchair nanoribbon in a magnetic field and with the gap parameter.
Methodology: This is an applied study in terms of type and a cognitive study in terms of approach. Here, a Hamiltonian tight-binding model is used to define the dynamics of the electrons in the device. Then, the energy bands of this sample are obtained by Hamiltonian diagonalization. The density of the energy states of the device has been obtained by using these energy bands.
Findings: Finally, the magnetic susceptibility and thermal capacity were obtained by integrating the energy on the state density and Dirac Fermi functions. The numerical results of the thermal capacity and magnetic susceptibility were obtained per various temperatures, various gap parameters, and various chemical potentials and their various widths.
Conclusion: It could be concluded from the present study that the thermal capacity of the magnetic susceptibility of armchair nanoribbon is influenced by the width of the armchair nanoribbon, chemical potential, and the energy gap parameter. Changes in the energy gap parameter, chemical potential, and the nanoribbon width lead to significant changes in the states and magnetic susceptibility of the armchair nanoribbon sample.

Keywords: Armchair, nanoribbon, magnetic susceptibility

Introduction

Many unique properties of nanomaterials are due to the high surface-to-volume ratio of nanoparticles or the long grain boundaries of nanostructured materials compared to ordinary materials. In a nanostructured material, lots of atoms (more than 49%) are in the grain boundaries [1].
Structures with 100-1 nm dimensions are taken into account in terms of (NMs). Due to the high surface-to-volume ratio and the possibility of quantum effects, the (NMs) behave completely different from their bulk counterparts. According to the European Commission (2016), a (NMs) is defined as "a natural, incidental or manufactured material containing particles, in an unbound state or as an aggregate or as an agglomerate and where, for 50 % or more of the particles in the number size distribution, one or more external dimensions is in size range 1 - 100 nm [2]." Although there are various types of (NMs), more varieties are expected to emerge in the future. In the meantime, currently, according to their structures, they are categorized as (i) carbon-based, (ii) metal, (iii) dendrimers, and (IV) composites [3].
Carbon-based (NMs) have been considered in the scientific and engineering community because of their unique physical, chemical, optical, mechanical, and thermal properties. Carbon-based (NMs) are usually

constructed in nanoparticles, hollow spheres, ellipses, platelets, or tubes. Carbon nanotubes (cylindrical) are usually produced by arc discharge or chemical deposition of graphite vapor [4]. In terms of hardness and flexibility modulus, carbon nanotubes are considered the most durable and rigid materials. A unique chain of carbon-carbon covalent bonds makes them extremely strong materials. Graphene is a carbon layer with the thickness of an atom arranged in a hexagonal lattice with excellent heat and electrical conductivity and optical transparency in the infrared and visible range. In addition, graphene is a very attractive option for various applications considering its strong and flexible properties and ability to link other elements (e.g., gases and metals) [5].

The effect of (NMs) on human cells has been investigated to understand its basic aspects. Negvin et al. (2015) found that the quantum point of cadmium telluride $(CdTeQD)$ can cause toxicity to cancer cells, hepatic cells, and $HepG2$ cells in humans through changing the morphology and structure of mitochondria. In addition, such nanostructures can reduce their capacity and stimulate biogenesis. $CdTe\text{-}QDs$ are suspected to affect the mitochondrial membrane potential strongly and cellular respiration, increase intracellular calcium levels and decrease adenosine triphosphate synthesis. These findings could prove that the human system may be severely damaged if exposed to high blood pressure. [3]

In the nanotechnology literature, nanostructures are synonymous with nanomaterials and are described as materials in which one of the sides is at the nanoscale (preferably 1 - 100 nm), which results in specific physical and chemical properties. In the meantime, nanostructures or, in other words, nanostructured materials are a group of nanomaterials that have special structures and properties. Nanostructured materials are polycrystalline bulk materials with a 1 – 100 nm grain size. It can be stated that nanoparticles are components of nanostructured materials. As mentioned, due to the high surface-volume ratio of nanoparticles, these materials tend to agglomerate or aggregate and react with the environment [6].

Since environmental impacts cannot be clearly identified due to large variables (e.g., detection, low detection limit, and unknown environmental concentrations), it is not easy to conclude environmental impacts and environmental stability. Even a slight change in chemical structure can fundamentally alter their properties and turn them into toxic compounds [7]. According to the US Environmental Protection Agency, "NMs are highly toxic due to their unique chemical properties, high reactivity, and insolubility in liquids." Since (NMs) are highly reactive, their properties in the environmental samples may alter the aggregation and analysis of samples. Identification of NMs between the samples is sometimes difficult. Scientists have recently investigated the environmental impacts of Ag_2S. It was found that plants may use nanosilver if it is present in the soil [8].

One of the important objectives of nanotechnology is the achievement of the electronic and structural properties of materials. This is one of the most important problems of today's research. Researchers have used theoretical calculations considering the complexities of the devices in the nanoscale. Most of the physical devices are in the form of many-particle devices, and each many-particle device incorporates lots of similar or different particles which interact with each other. At the microscale, each material may be a many-particle device in itself [9].

Materials and methods

Electron density in a specific position in the space is $n(r)$ which can be rewritten based on the one-electron wave functions [10]:

$$n(r)=2\sum_{i}\psi_i^*(r)\psi_i(r) \quad (1)$$

In order to facilitate calculations considering the increased number of particles (electrons and ions), as well as the complexity of the quantum devices in the solid object, we are to use the second quantification approach as well as the tight-binding approximation in our equations to obtain the Hamiltonian of the system. Using the tight-binding approximation, the Hamiltonian only consists of two terms of the electron kinetic energy and the electrostatic electron-ion potential. We require a complete Hilbert space to solve the Schrodinger equation and investigate the electron energy spectrum. Therefore, the atomic orbital wave functions (Wannier wave functions) should be described. The Wannier wave function indicates that in the wave functions resulting from solving the Schrodinger equation, the electron is bound to only one ion [11].

$$\left|\varphi_i\right\rangle=\left|\varphi\left(r-R_i\right)\right\rangle \quad (2)$$

Due to the completeness of the Hilbert space, which includes the atomic orbital wave functions, the wave functions and especially the Schrodinger equation functions of the real device may be found considering the linear composition of these atomic orbitals. Hybridization is the combination of atomic orbital wave functions used for finding the wave functions in which the electron is in front of several ions. This combined wave function is called the hybridization wave function. This combined wave function sandwiches the Hamiltonian between special atomic orbital functions $\left\langle\varphi_i\right|\left|H\right|\left.\varphi_j\right\rangle$, which gives the amplitude of the electron jump from one ion to another. In other words, the amplitude of the electron jump is from the i^{th} ion to the j^{th} one [12].

Hamiltonian of crystal

Considering the spin energy and ion potential of the ion, the Hamiltonian of an independent one-electron crystal is as follows:

$$H = \frac{p^2}{2m} + \sum_{i,\tau} V(r - R_{i\tau})$$

(3)

Writing the Hamiltonian in atomic orbital bases using the Schrodinger equation for Eq. (4) gives a non-diagonal matrix diagonalized by changing the basis and using indirect space. In the first step, we propose the following wave function to solve the eigenvalue equation of $H\psi = E\psi$:

$$\psi_\tau(k,r) = \frac{1}{\sqrt{N}} \sum_i e^{ik.R_i} \varphi_\tau(r - R_i)$$

(4)

$\varphi_\tau(r - R_i)$ is the atomic orbital wave function of the electron is in the presence of ions located in the R_i unit cell and the τ basis, which represents a basis conversion. In other words, we have translated from the i atomic orbital basis in direct space to the τ basis and the wave vector k, where k is the wave vector in the inverse space. Now, we prove that Hamiltonian is on the index k at this diameter basis, that is

$$H_{kk'}^{\tau\tau'} = \langle \psi_\tau(k,r) | H | \psi_{\tau'}(k',r) \rangle = \delta_{kk'} E_n$$

$$\langle \psi_\tau(k,r) | H | \psi_{\tau'}(k',r) \rangle = \int d^3 r \psi_\tau^*(k,r) \left(\frac{p^2}{2m} + \sum V(r - R_{i\tau}) \right) \psi_{\tau'}(k',r)$$

(5)

The above integral is on the variable of electron location, but using Eq. (5), the element of Hamiltonian matrix in Bloch space can be written as follows [13]

$$\langle \psi_\tau(k,r) | H | \psi_{\tau'}(k',r) \rangle = \frac{1}{N} \sum_{i,j} e^{-ik.R_i} e^{ik'.R_j} \langle \varphi_\tau(r - R_i) | H | \varphi_{\tau'}(r - R_j) \rangle$$

(6)

In a unit cell, the starting basis atom and the ending base atom are equivalent to the starting basis atom and the ending basis atom in another unit cell, so this variable alteration is possible. In other words, the location difference is only important at the starting and ending unit cells, not at the origin. So the Hamiltonian form in the new basis is as follows (7):

$$H_{kk'}^{\tau\tau'} = \sum_\Delta e^{ik.\Delta} H^{\tau\tau'}(\Delta) \delta_{kk'}$$

$$\frac{1}{N} \sum_i e^{i(k'-k).R_i} = \delta_{kk'}$$

(7)

Eq. (7) is the Hamiltonian matrix element between a unit cell at the origin and a unit cell at the τ location. Alternatively, we take one of the unit cells as the origin, and the rest of the unit cells are constructed by the translation vector τ.

The Hilbert space created by the bandwidth functions diagonalizes the crystal's Hamiltonian in the tight-binding approximation, that is:

$$\langle \psi_n(k) | H | \psi_{n'}(k) \rangle = E_n(k) \delta_{nn'}$$

(8)

Therefore, the wave functions of the band structure that could completely diagonalize Hamiltonian are written as follows [1]:

$$\psi_n(k) = \sum_{\tau=1}^m C_{n\tau}(k) \psi_\tau(k) = \frac{1}{\sqrt{N}} \sum_{\tau,i} C_{n\tau}(k) e^{ik.R_i} \varphi_\tau(r - R_i)$$

(9)

The following steps must be taken in order to obtain the eigenvalues of a crystal

1. Selecting the reference unit cell
2. Determining the number of atomic bases
3. Obtaining the Hamiltonian matrix elements between the reference unit cell and the unit cells in Δ, that is $H^{\tau\tau'}(\Delta)$ (amplitude of electron jump between two atoms at two wave bases in two neighboring unit cells)
4. Formulating the equation

$$H^{\tau\tau'} = \sum_\Delta e^{ik.\Delta} H^{\tau\tau'}(\Delta) \quad (10),$$

5. Diagonalization of the obtained matrix; obtaining eigenvalues and eigenvectors.

The number of terms in Eq. (10) depends on the number of cells in the neighboring unit. Also, the dimensions of the matrix obtained from this equation depend on the number of atomic bases. The closest neighbor approximation is used to calculate the Hamiltonian eigenvalues and eigenvalues of a crystal. All amplitudes of the distant atom jumps in the nearest neighbor approximation are considered zero. The nearest neighbor approximation makes zero some of our matrix elements [14].

Analysis of the ribbon structure of armchair nanoribbon

The analytical solution and wave function of the armchair nanoribbon are provided based on the tight-binding approximation. We may realize that the wave function is discrete in the finite direction. This discrete wave function emerges from underneath various ribbons as an index. The structure of the armchair nanoribbon includes two atoms, and two hard walls $(j = 0, n+1)$ apply on the edges. This is shown in Fig.1. The unit cell in this figure includes N atoms which consist of A and B sub-lattice atom types [15].

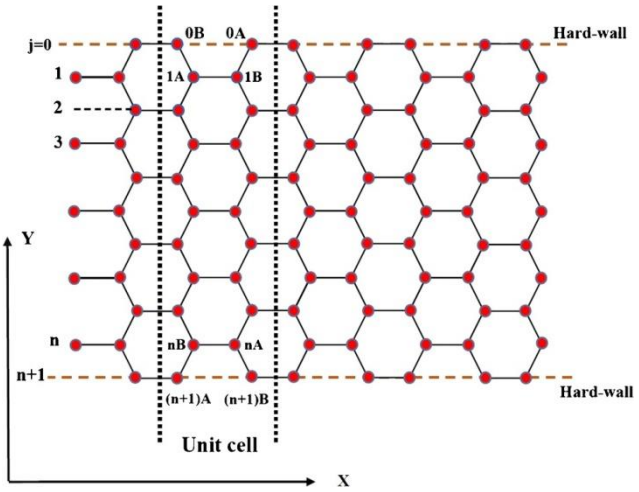

Figure 1. Structure of the armchair nanoribbon includes two atoms and two hard walls applied on the edges

In the tight-binding model, the Bloch wave functions, which are related to the A and B sublattice atoms, could be written as follows

$$\left|k_x, p, A\right\rangle = \frac{1}{N_A}\sum_{i=1}^{n}\sum\nolimits_{x_{Ai}} \exp(ik_x.x_{Ai})\phi_A(i)\left|A_i\right\rangle$$

$$\left|k_x, p, B\right\rangle = \frac{1}{N_B}\sum_{i=1}^{n}\sum\nolimits_{x_{Bi}} \exp(ik_x.x_{Bi})\phi_B(i)\left|B_i\right\rangle$$

(11)

Where, $\phi_A(i)$ and $\phi_B(i)$ are functions that should be determined through the boundary conditions. $\left|A_i\right\rangle$ and $\left|B_i\right\rangle$ are the wave functions of the atomic orbital of the electron in proximity to the A and B sublattice atoms at two atomic bases. Boundary conditions are used to obtain $\phi_A(i)$ and $\phi_B(i)$ and two boundaries of $(j=0, n+1)$ are introduced:

$$\phi_A(j=0)=\phi_B(j=0)=0$$
$$\phi_A(j=n+1)=\phi_B(j=n+1)=0 \qquad (12)$$

Replacing $\phi_A(i)=\phi_B(i)=\sin(\frac{\sqrt{3}q_y a}{2}i)$ in Eq. 12, we have

$$\phi_A(i)=\phi_B(i)=\sin(\frac{\sqrt{3}}{2}q_y ai) \Rightarrow \phi_A(n+1)=\phi_B(n+1)=\sin(\frac{\sqrt{3}}{2}q_y a(n+1))$$

$$\frac{\sqrt{3}}{2}q_y a(n+1)=p\pi \Rightarrow q_y=\frac{2}{a\sqrt{3}}\frac{p\pi}{n+1} \qquad p=1,2,...$$

$$\Rightarrow \phi_A(i)=\phi_B(i)=\sin(\frac{p\pi}{n+1}i)$$

(13)

a is the length of the atomic bonds in the A and B sublattice. To obtain the normalized coefficients of $\mathrm{N_A}$ and $\mathrm{N_B}$, we use the normalization condition

$$\left\langle k_x, p, A\middle| k_x, p, A\right\rangle = \left\langle k_x, p, B\middle| k_x, p, B\right\rangle = 1 \Rightarrow \mathrm{N_A}=\mathrm{N_B}=\sqrt{\frac{\mathrm{N_x}(n+1)}{2}}$$

(14)

$\mathrm{N_x}$ is the number of unit cells along the x. the Eq. (11) is rewritten as follows

$$\left|k_x, p, A\right\rangle \sqrt{\frac{2}{N_x(n+1)}}\sum\nolimits_{x_{Ai}}\sum_{i=1}^{n} e^{ik_x x_{A_i}} \sin(\frac{\sqrt{3}q_y a}{2}i)\left|A_i\right\rangle$$

$$\left|k_x, p, B\right\rangle = \sqrt{\frac{2}{N_x(n+1)}}\sum\nolimits_{x_{Bi}}\sum_{i=1}^{n} e^{ik_x x_{B_i}} \sin(\frac{\sqrt{3}q_y a}{2}i)\left|B_i\right\rangle$$

(15)

The general band wave function of the system could be obtained through the linear combination of $\left|k_x, p, A)\right\rangle$ and $\left|k_x, p, B)\right\rangle$ as follows

$$\left|\psi\right\rangle = C_A\left|k_x, p, A\right\rangle + C_B\left|k_x, p, B\right\rangle \Rightarrow$$

$$C_A\left(\sqrt{\frac{2}{N_x(n+1)}}\sum\nolimits_{xA_i}\sum_{i=1}^{n} e^{ik_x xA_i} \sin\left(\frac{\sqrt{3}q_y a}{2}i\right)\left|A_i\right\rangle\right) +$$

$$C_B\left(\sqrt{\frac{2}{N_x(n+1)}}\sum\nolimits_{xB_i}\sum_{i=1}^{n} e^{ik_x xB_i} \sin\left(\frac{\sqrt{3}q_y a}{2}i\right)\left|B_i\right\rangle\right)$$

(16)

Assuming isotropy, we consider the electron jump integral as $t_{i,j}=t$ in the armchair nanoribbon. Replacing Eq. 16 and the system's Hamiltonian in the Schrodinger equation, the following matrix could be obtained:

$$\begin{bmatrix} \langle k_x,p,A|H|k_x,p,A\rangle & \langle k_x,p,A|H|k_x,p,B\rangle \\ \langle k_x,p,B|H|k_x,p,A\rangle & \langle k_x,p,B|H|k_x,p,B\rangle \end{bmatrix}\begin{bmatrix} C_A \\ C_B \end{bmatrix} = E\begin{bmatrix} C_A \\ C_B \end{bmatrix}$$

$$\Rightarrow \begin{bmatrix} \Delta & F \\ F^* & -\Delta \end{bmatrix}\begin{bmatrix} C_A \\ C_B \end{bmatrix} = E\begin{bmatrix} C_A \\ C_B \end{bmatrix} \rightarrow \begin{bmatrix} \Delta - E & F \\ F^* & -\Delta - E \end{bmatrix}\begin{bmatrix} C_A \\ C_B \end{bmatrix} = 0$$

(17)

Furthermore, the final energy form of the armchair nanoribbon is as follows:

$$E_+(k_x,p) = +\sqrt{\Delta^2 + t^2(1+4\cos^2(\frac{p\pi}{n+1}) + 4\cos(\frac{p\pi}{n+1})\cos(\frac{k_x}{2}a)}$$

$$E_-(k_x,p) = -\sqrt{\Delta^2 + t^2(1+4\cos^2(\frac{p\pi}{n+1}) + 4\cos(\frac{p\pi}{n+1})\cos(\frac{k_x}{2}a)}$$

(18)

Calculation of Hamiltonian functions

The following relation holds for Hamiltonian of the armchair nanoribbon function:

$$\begin{bmatrix} \Delta & F \\ F^* & -\Delta \end{bmatrix}\begin{bmatrix} C_A \\ C_B \end{bmatrix} = +\sqrt{\Delta^2 + FF^*}\begin{bmatrix} C_A \\ C_B \end{bmatrix} \rightarrow \begin{matrix} \Delta C_A + FC_B = +\sqrt{\Delta^2 + FF^*}C_A \\ F^*C_A - \Delta C_B = +\sqrt{\Delta^2 + FF^*}C_B \end{matrix}$$

(19)

Using Eq. 19, we have

$$C_B = \frac{\left(\sqrt{\Delta^2 + FF^*} - \Delta\right)}{F} C_A$$

(20)

The general wave function is thus obtained, where

$$|\psi\rangle = C_A|k_x,p,A\rangle + C_B|k_x,p,B\rangle = C_A\left\{|k_x,p,A\rangle + \frac{\left(\sqrt{\Delta^2 + FF^*} - \Delta\right)}{F}|k_x,p,B\rangle\right\}$$

(20)

Therefore, the wave functions will be obtained as follows in the band index space, and the following solutions will be obtained after their normalization:

$$|\psi_{(k_x,p)}\rangle_\pm = \frac{1}{\sqrt{2 + \frac{2}{FF^*}\left(\Delta^2 - \Delta\sqrt{\Delta^2 + FF^*}\right)}}\left\{|k_x,p,A\rangle \pm \left(\frac{\sqrt{\Delta^2 + FF^*} - \Delta}{F}\right)|k_x,p,B\rangle\right\}$$

(21)

Where ± indicates the conduction and capacity bands [47]

Density of states of armchair nanoribbon

Energy state density is the most important quantifiable and measurable quantity in experiments. The density of states $D(E)$ is used to indicate the number of states of electron energy in the conduction band. In other words, $D(E)dE$ shows the number of states of the electron energy, the energy level of which is in the interval E to $E + dE$ per energy range unit dE. The equation for the density of states is as follows:

$$D(E) = \sum_{n,k} \delta(E - E_n(k_x, p))$$

(22)

Where, $\delta(E - E_{n,k})$ is an indication of the number of states, where the corresponding energy is in the E interval. If the density of states equals zero at the Fermi energy level or the chemical potential,the device adopts a nonmetallic property, and if it does not equal zero $D(E = \mu = \varepsilon_F) \neq 0$, the device takes a metallic or conductive property. It should be noted that the density of states is related to the band structure as follows:

$$D(E) = -\frac{1}{2\pi N}\,\mathrm{Im}\sum_{k_x,p,n=\pm}\frac{1}{E - E_n(k_x,p) + i0^+}$$

(23)

Magnetic susceptibility of armchair nanoribbon in the presence of magnetic field

Magnetic susceptibility is a fundamental characteristic of materials, and when it is located in an external magnetic field, it will change it in the surrounding and nearby areas. Magnetic susceptibility is defined as follows:

$$\chi = \frac{M}{B}$$

(24)

Where B is the intensity of the magnetic field, M is the magnetic moment per unit volume (magnetization), and χ is the magnetic susceptibility, which is a dimensionless quantity. In case $\chi \succ 0$, the material is paramagnetic, which strengthens the magnetic field. Also $\chi \prec 0$, the material is diamagnetic, which weakens the magnetic field. In this thesis, the magnetic susceptibility is stated as follows using the Kubo formula

$$\chi = -2\mu_B \int dE\, D(E)\frac{\partial f(E)}{\partial E}$$

(25)

This equation indicates that the magnetic susceptibility could be calculated by the density of states of a material [16].

Results

Magnetic susceptibility of armchair nanoribbon

Using the density of states of the nanoribbon, the magnetic susceptibility of graphene-like armchair nanoribbons can be plotted based on energy according to the following diagrams.

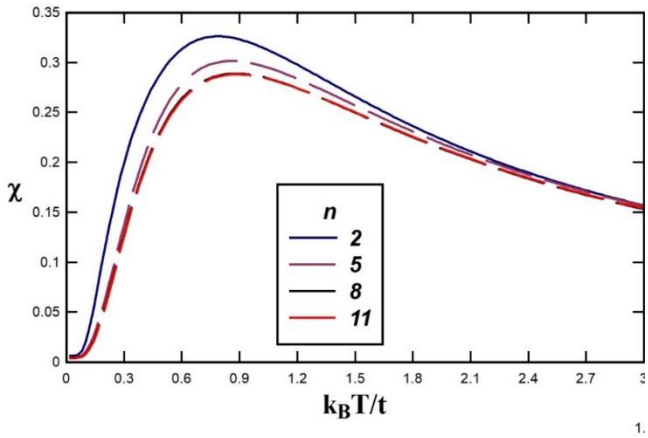

Diagram 1. Magnetic susceptibility of graphene armchair nanoribbons based on temperature for different widths

Dia. (1) shows the temperature behavior of an armchair nanoribbon in the zero-gap parameter for different widths at zero chemical potential. We may realize from this figure that there is a peak in the temperature behavior o this thermodynamic quantity, the height of which decreases with the increase in the width of the nanoribbon. Also, a downward behavior is observed at high temperatures for all nanoribbon widths due to the classical property of electrons with temperature. At low temperatures, the quantum effects of the inter-ribbon transition increase the susceptibility temperature. At relatively high temperatures, almost all susceptibility diagrams overlap.

The effect of the gap parameter on the temperature behavior of magnetic susceptibility for the metal state with the width of n = 4 is shown in Dia. (2). The diagram indicates that with the increase in the gap, the location of the peak in the magnetic susceptibility shifts to the high-temperature values parameter. This feature is due to the increase in the width of the gap within the density of states so that the electrons are excited by increasing the gap parameter at a higher temperature. In addition, Dia. (2) shows that the magnetic susceptibility decreases with an increasing gap at a constant temperature.

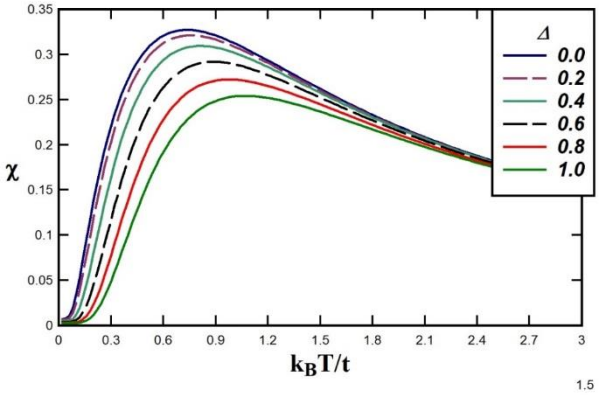

Diagram 2. Magnetic susceptibility of graphene armchair nanoribbons in terms of temperature for the width of n = 4 in gap parameters of different energy levels

In Dia. (3), the magnetic susceptibility is zero for various chemical potential values in metal nanoribbon with the width of n = 4 and the gap parameter. It is clear from the figure that at low-temperature values, an upward behavior is observed for magnetic susceptibility at all values of chemical potential, so the susceptibility increases with increasing chemical potential. This is due to the increase in the inter-ribbon transition rate with increasing chemical potential or electron concentration. So, various graphs almost overlap for different amounts of chemical potential at high temperatures. Furthermore, a downward trend with temperature is observed for magnetic susceptibility.

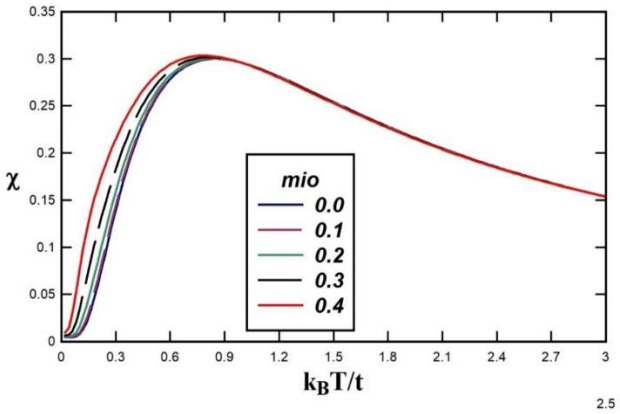

Diagram 3. Magnetic susceptibility of graphene armchair nanoribbon based on temperature using the chemical potential for the width of n = 4

Density of armchair nanoribbons

Dia. (4) shows the density of energy states of armchair nanoribbons with the width of n = 4 and different values of the gap parameter. The diagram shows that with an increase in the gap parameter, the gap width of the energy density is increased.

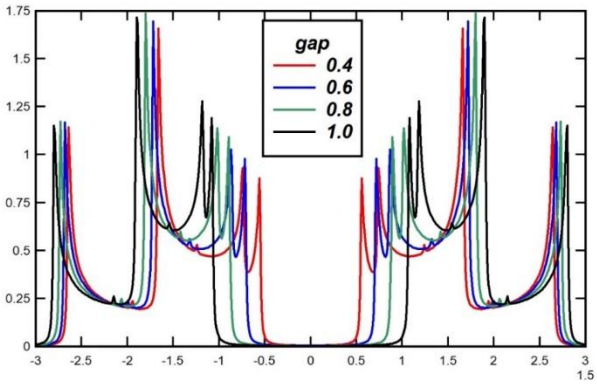

Diagram 4. Density of states (DOS) of armchair nanoribbons based on (E) for the width of n = 4

Conclusion

In this study, we investigated the temperature behavior of the magnetic susceptibility of the graphene-like armchair nanoribbon lattice in the presence of a magnetic field and the gap parameter. A Hamiltonian Hubbard model, including terms for the kinetic and potential energies, was used to describe the dynamics of the electrons. We obtained the Hamiltonian of the device using the second quantization, and then, using the electron energy bands,

we studied and investigated the density of states of electrons and the magnetic susceptibility of the sample armchair nanoribbon. Changing the gap energy parameters and the width of the nanoribbon, the effects of these quantities on the magnetic susceptibility could be analyzed. Also, the effects of electron injection as the numerical changes in the chemical potential on magnetic susceptibility were studied in the Hamiltonian model.

According to the results, the magnetic susceptibility indicates a peak in the temperature behavior of this thermodynamic quantity, where the height of the peak decreases with the increase in the width of the nanoribbon. Also, at high temperatures, a downward trend in observed due to the classic temperature behavior of electrons in all widths of the nanoribbon. At low temperatures, the quantum effects of the inter-ribbon transition increase the temperature-related susceptibility. At relatively high temperatures, almost all susceptibility diagrams overlap.

In addition, the effect of the gap parameter on the temperature behavior-related magnetic susceptibility was investigated at the metal state with the width of n = 4. According to the results, with the increase in the gap parameter, the peak of the magnetic susceptibility shifts to high-temperature values. This is due to the increase in the width of the gap within the density of states so that with an increase in the gap parameter at higher temperatures, the electrons are excited. Also, the magnetic susceptibility decreases with increasing gap parameters. In the investigation of the density of states of the armchair nanoribbons, it was found that with an increase in the gap parameter, the density of the energy gap increases.

Acknowledgments: Eshragh Company

Conflict of Interest: None

Financial Support: None

Ethics Statement: None

References

1. R.Egger, and H.Schoeller, RKKY interaction and Kondo screening cloud for strongly correlated electrons, Physical Review B, 54-16337(1996).
2. K. S. Novoselov, A. K. Geim, S. V. Morozov, D. Jiang, Y.Zhang, S. V. Dubonos, I. V. Grigorieva, and A.A. Firsov, Electric field effect in atomically thin carbon films, Science **306,** 666 (2004).
3. E.kabir et al.Environmental impacts of nanomaterials.Journal of Environmental Management 225 (2018) 261-271
4. Y. Hernandez, V. Nicolosi, M. Lotya, F. M. Blighe, Z. Sun, S. De, I. T. Mc Govetn, B. Holland, M. Byrne, Y. K. Gun'Ko, J.J. Boland, P.Niraj, G. Duesberg, S. Krishnamurthy, R. Goodhue, J. Hutchison, V. Seardaci, A.C Ferrari and J. N Coleman, High-yield production of graphene by liquid-phase exfoliation of graphite, Nat.
5. U. Khan, A. O' Neill, M. Lotya, S. De and J. N. Coleman, High-concentration solvent, exfoliation of graphene, Small **6,** 864 (2010).
6. A.G. Cano-Marquez, F.J. Rodriguez-Macias, J. Campos-Delgado, C.G. EspinosaGonzalez, F. Tristan-Lopez, D. Ramirez-Gonzalez, D.A. Cullen, D.J. Smith, M. Terrones, Y.I. Vega-Cantu, Nano Lett,1527-1533 (2009).
7. S. R. Power, F. S. M. Guimarães, A. T. Costa, R. B. Muniz, and M. S. Ferreira, Dynamic RKKY interaction in graphene, Phys. Rev. B, Vol. 85, pp. 195411, (2012).
8. G. Dresselhaus P. Eklund M. Dresselhaus, Science of Fullerenes and Carbon Nanotubes, Elsevier Science, 965, (1996).
9. L. Jiao, X. Wang, G. Diankov, H. Wang, H. Dai, Nature 458 ,877-88 (2009).
10. J. Wiley, S, Inc. Density Functional Theory,(2009)p,22-25
11. D.B. Shinde, J. Debgupta, A. Kushwaha, M. Aslam, V.K. Pillai, J. Am. Chem. Soc. 133,4168–4171(2011).
12. H Imamura, P. Bruno, and Y.Utsumi Twisted exchange interaction between localized spins embedded in a one- or two-dimensional electron gas with Rashba spin-orbit coupling, Physical Review B, 69-121303(2004).
13. L. Jiao, L. Zhang, L. Ding, J. Liu, H. Dai, Nano Res. 3, 387–394(2010).
14. M.Saiz-Bretin, A.V.Malyshev, F. Dominguez-Adame, D.Quigley, R.A.Ro¨mer, D.Quigley, Lattice thermal conductivity of gtaphene nanostructures, Carbon (2017)
15. H. Rezania, A. Abdi. Dynamical and Static Spin Susceptibilities of Doped Gapped Graphene Nanoribbon Due to Local Electronic Interaction,(2017)
16. K. Kim, A. Sussman, A. Zettl, ACS Nano 4, 1362-1366(2010).